Miscible Polyisoprene/Polystyrene Blends: Distinct Segmental Dynamics but Homogeneous Terminal Dynamics

Yiyong He, T. R. Lutz, and M. D. Ediger*

Department of Chemistry, University of Wisconsin−Madison, Madison, Wisconsin 53706

Marinos Pitsikalis and Nikos Hadjichristidis

Department of Chemistry, University of Athens, Panepistimiopolis, Zografou 15771 Athens, Greece

Ernst D. von Meerwall

Department of Physics and Maurice Morton Institute of Polymer Science, University of Akron, Akron, Ohio 44325

Received March 10, 2005; Revised Manuscript Received May 9, 2005

ABSTRACT: The segmental and terminal dynamics of the individual components in miscible blends of polyisoprene (PI) and polystyrene (d_3PS) were characterized over a wide temperature range. Though the system has a large positive Flory−Huggins interaction parameter $\chi \sim 0.1$, it is miscible in the temperature range of study due to low molecular weight. ^{13}C and ^{2}H NMR relaxation measurements were performed to extract the segmental relaxation times. Pulse-gradient spin-echo NMR was used to determine the center-of-mass diffusion coefficients. Though the segmental dynamics of PI and PS components differ by more than 2 decades at $T_g + 50$ K in the blends, their terminal dynamics (in terms of monomeric friction coefficients) are essentially identical. We know of no other system with this behavior. The distinct component segmental dynamics can be reasonably interpreted by the Lodge/McLeish model. The unusual homogeneous terminal dynamics may be due to a large thermodynamic barrier to diffusion in this system. The monomeric friction coefficients are well reproduced by the Gordon−Taylor mixing rule.

I. Introduction

The dynamics of miscible polymer blends are important in understanding a wide range of phenomena including the processing and rheological response of polymer mixtures, transport in such mixtures, and the kinetics of phase separation. In each of these areas, the macroscopic response of the polymer mixture reflects the combined contribution of the components. It is necessary to understand not only the segmental and terminal dynamics of individual components in the mixtures but also the "mixing rules" that determine the macroscopic response.

Work in the past two decades has revealed that dynamics in miscible polymer mixtures are significantly more complex than in undiluted homopolymers. The time−temperature superposition principle that is reasonably successful in describing the rheology of homopolymer melts has been shown to fail dramatically for many blend systems, and very broad calorimetric glass transitions are commonly observed.[1−4] This interesting complexity, and the importance of polymer mixtures, have spurred a great deal of recent research.[4−28]

Significant progress has been made toward understanding the segmental dynamics in miscible polymer blends. The component segmental dynamics have been separately characterized in a number of polymer blends using NMR,[5,10,15−17] dielectric relaxation,[6,12,14,20] and thermally stimulated depolarization currents.[27] Collectively this work indicates that, in most systems, the segmental dynamics of the components are distinct and have their own temperature dependences, even though the two components are well-mixed on a molecular level. A good example is the miscible blend system, polyisoprene/poly(vinyl ethylene) (PI/PVE), which has a slightly negative Flory−Huggins interaction parameter χ.[29] The segmental relaxation times of the two components differ by as much as 10^4, and the effective glass transition temperature (T_g) associated with each component differs by more than 20 K.[5] In the Lodge/McLeish model,[30] these distinct segmental dynamic behaviors are explained by chain connectivity.[5] This model assumes that the segmental relaxation times of a given polymer segment depend on the composition of a local volume (with a size equal to the Kuhn length) rather than the bulk composition. In such a small volume, the contribution of segments that are directly bonded to the segment of interest is significant. Thus, any given segment will be in an environment that is rich in units of the same kind and thus retains part of its intrinsic dynamic features. The Lodge/McLeish model has been shown to account for many experimental results in a qualitative manner, and in several cases, it is able to provide a quantitative description.[11,26,31,32]

The terminal dynamics of the components in miscible polymer blends are less well understood. Experimental information, from either the monomeric friction coefficient ζ or the center-of-mass diffusion coefficient D, has been obtained for a number of miscible blends, including PI/PVE,[11,33] polybutadiene/poly(vinyl ethylene) (PB/PVE),[21] polystyrene/tetramethylbisphenol A polycarbonate (PS/TMPC),[19] polystyrene/poly(xylenyl ether) (PS/PXE),[18] and poly(ethylene oxide)/poly(methyl methacrylate) (PEO/PMMA).[2,34] The data as a whole indicate significant complexity. In some cases, e.g., PB/PVE, PS/TMPC, PEO/PMMA (20/80), the terminal dynamics of the two components (characterized by

* Corresponding author. E-mail ediger@chem.wisc.edu.

10.1021/ma0505225 CCC: $30.25
Published on Web 06/11/2005

monomeric friction coefficient ζ) differ both in value and in temperature dependence; in other systems (PI/PVE and PS/PXE), the two components have significantly different ζ values but similar temperature dependences. Efforts have been made toward predicting the component terminal dynamics in miscible blends,[35] either by applying mixing rules to the homopolymer dynamics[25,36] or by relating the terminal dynamics to the component segmental dynamics.[11,23,24,26]

To make practical predictions about a range of properties for miscible polymer mixtures, we need to understand both the segmental and terminal dynamics of such mixtures. It is reasonable to assume that these are connected problems; i.e., we expect that understanding segmental dynamics will be of some use in predicting terminal dynamics. For homopolymers, it is well established that in most systems the segmental and terminal dynamics exhibit the same temperature dependence well above T_g.[37−39] This is consistent with the view that the segmental motions are the fundamental kinetic process which drive all other processes on longer length and time scales. While the simple relationship between segmental and terminal dynamics observed in homopolymer melts is consistent with data on one miscible blend system (PI/PVE),[11] it does not work for a second system (PB/PVE).[26]

To further investigate the connection between segmental and terminal dynamics, we present here measurements of both quantities for both components in a miscible blend of polyisoprene and polystyrene (PI/PS). NMR relaxation and diffusion experiments were performed on isotopically labeled polyisoprene/polystyrene (PI/PS) blends over a wide composition and temperature range. NMR methods based upon isotopic labeling allow the separate observation of the dynamics of each component. We measured the ^{13}C spin−lattice relaxation time (T_1) and nuclear Overhauser effect (NOE) for PI, and ^2H T_1 for PS, and used these data to obtain the segmental correlation times for each component. Pulse-gradient spin-echo (PGSE) NMR diffusion experiments in the proton resonance were performed on the same set of samples.

Though the segmental dynamics of the PI and PS components differ by more than a factor of 100 at T_g + 50 K, the terminal dynamics of the two components (in terms of the monomeric friction coefficient ζ) are essentially identical. We know of no other system showing these features. The distinct component segmental dynamics can be reasonably interpreted by the Lodge/McLeish model. The unusually homogeneous terminal dynamics are possibly due to a large thermodynamic barrier to diffusion in this system. The monomer friction coefficients are well described by the Gordon−Taylor mixing rule.

II. Experimental Section

Materials Synthesis and Characterization. All polymers were synthesized through anionic polymerization. ^{13}C-labeled isoprene monomers were purchased from Isotrading VOF. Both backbone deuterated and perdeuterated styrene monomers were purchased from Cambridge Isotope Laboratories, Inc. The solvent (benzene) and the monomers were purified according to standard methods for anionic polymerization.[40] *sec*-Butyllithium (*sec*-BuLi) was prepared under vacuum by the reaction of the corresponding chloride with lithium dispersion. The synthesis was performed in vacuo in all-glass reactors equipped with break-seals and constrictions. The polymerizations were conducted in benzene at room temperature. The living polymers were terminated by degassed methanol. A considerable amount of lithium salts was produced after the termination reaction due to the low molecular weight of the samples. Therefore, the samples were dissolved in toluene and the salts were extracted several times with distilled water. The organic phase was dried over anhydrous sodium sulfate, and then the polymers were precipitated in methanol and dried under vacuum. Transparent samples were obtained.

Table 1. Characterization of PI and PS Homopolymers

samples	M_n (kg/mol)	M_w/M_n	T_g (K)
PI[a]	0.9	1.37	190
d_3PS	1.6	1.28	320
d_8PS	1.7	1.20	319

[a] 68% *cis*-1,4, 20% *trans*-1,4, 12% 3,4.

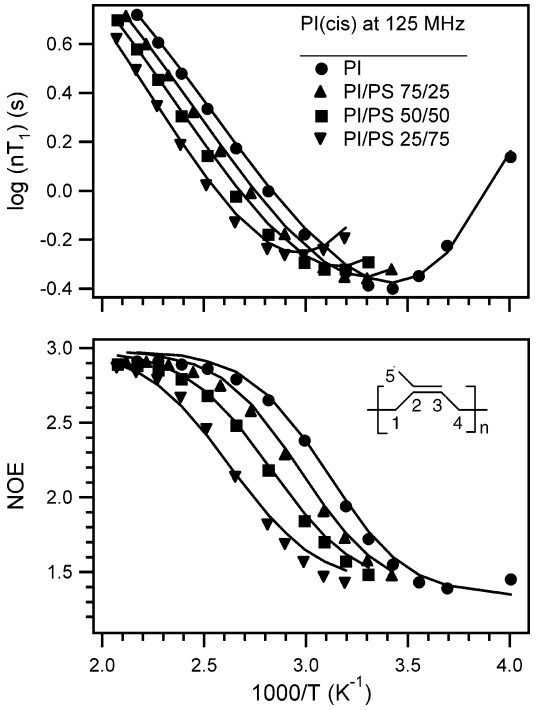

Figure 1. ^{13}C T_1 and NOE for C1 carbon of *cis*-PI as a homopolymer and in three PI/PS blends at 125.8 MHz. The solid curves are fits using the mKWW autocorrelation function and VTF temperature dependence. The fit parameters are listed in Table 2.

The molecular weights and their distributions were characterized by size exclusion chromatography (SEC). The experiments were conducted at 40 °C using a modular instrument consisting of a Waters model 510 pump, a Waters model U6K sample injector, a Waters model 401 differential refractometer, a Waters model 486 UV spectrophotometer, and a set of 4 μ-Styragel columns with a continuous porosity range from 10^6 to 500 Å. The columns were housed in an oven thermostated at 40 °C. THF was the carrier solvent at a flow rate of 1 mL/min. The sample molecular weights were analyzed using PI and PS calibration curves, covering the molecular weight range from 1000 to 5000 g/mol. The microstructure information was obtained by NMR.

Differential scanning calorimetry measurements were carried out on a Netzsch 200 DSC. T_g is taken as the midpoint of the transition trace in heating with a scan rate of 10 K/min after cooling the samples at the same rate from well above T_g.

All the characterization information is listed in Table 1. The prefixes d_3 and d_8 denote backbone deuteration and perdeuteration, respectively. The PI samples have 66% ^{13}C enrichment for C1 carbon and 33% ^{13}C enrichment for C5 carbon (see Figure 1).

Sample Preparation. Five samples were prepared for both NMR relaxation measurements and PGSE NMR diffusion

measurements: PI/d_3PS (wt %) 100/0, 75/25, 50/50, 25/75, 0/100. One additional sample, PI/d_8PS 25/75, was prepared for PGSE NMR diffusion experiments. The binary miscible blends were prepared by solvent-casting dilute cyclopentane solutions. First the two components were dissolved in cyclopentane in a glass vial to make a 10% solution. The blend solution was stirred for 2 h to ensure complete mixing. After ~90% of the solvent was removed by blowing N_2 gas onto the solution surface, the solution was transferred to a NMR tube and coated onto the wall of the tube. Vacuum was then applied for 72 h while holding the tube horizontally, allowing the remaining solvent to be removed. The resulting blend was subsequently heated to roughly T_g + 100 K and placed vertically to allow the sample flow to the bottom of the tube. Finally the sample was sealed under vacuum. The homopolymers were directly loaded into NMR tubes and sealed under vacuum.

The PI/PS blend samples are miscible above 303 K. The phase transition temperatures determined by observing cloud points are consistent with the phase diagram reported in the work of Semenov and co-workers, which is computed from a thermodynamic interaction parameter $\chi = -0.07 + 63/T$.[25] All measurements were done in the one-phase regime.

NMR Relaxation Measurements. Two different relaxation measurements, T_1 and NOE, were conducted over ~200 K temperature range, with the low-temperature limit of ~T_g + 50 K. Both NMR observables detect segmental dynamics as they are sensitive to the reorientation of backbone C−H or C−D bond vectors. T_1 was measured by the standard $\pi-\tau-\pi/2$ pulse sequence, waiting at least $8T_1$ between the acquisition and the next pulse. NOE was measured as the ratio of ^{13}C signal intensity of the spectrum with continuous decoupling to that with inverse-gated decoupling, waiting at least $10T_1$ between acquisitions. The number of scans used for signal averaging ranges from 8 to 128, depending on the sample and temperature. Averaged T_1 and NOE values, based on at least three runs, were used for further analysis at each temperature. Spectra were processed with line broadening equal to one-tenth of the line width of the spectra, followed by fitting the peak area as a function of delay time to a three-parameter exponential function. The uncertainty in T_1 is ±7% and in NOE is ±0.05. Measurements were performed on a Varian Inova-500 NMR spectrometer (500 MHz proton frequency) and a Bruker DMX-300 NMR spectrometer (100 MHz proton frequency). Temperature was controlled to ±0.5 K and calibrated to within an uncertainty of ±3 K using a combination of an ethylene glycol thermometer[41] and melting point standards. Several tests were performed to ensure that no detectable degradation took place during experiments.[42]

In this work, we selectively measured ^{13}C and ^{2}H resonance signals for PI and d_3PS, respectively. For PI, ^{13}C T_1 and NOE experiments were performed on the C1 methylene carbon (Figure 1) at ^{13}C frequencies of 25.1 and 125.8 MHz. *Cis* and *trans* isomeric resonance peaks are well resolved, and their T_1 and NOE were measured and analyzed separately. For d_3-PS, ^{2}H T_1 were measured for the backbone deuterons at ^{2}H frequencies of 15.3 and 76.8 MHz.

NMR Relaxation Mechanism and Segmental Correlation Time. For sp^3 carbons in polymers, dipolar interaction is the only significant relaxation mechanism for ^{13}C spin−lattice relaxation. The ^{13}C T_1 and NOE are given by[43−45]

$$\frac{1}{T_1} = Kn[J(\omega_H - \omega_C) + 3J(\omega_C) + 6J(\omega_H + \omega_C)] \quad (1)$$

$$\mathrm{NOE} = 1 + \frac{\gamma_H}{\gamma_C}\left[\frac{6J(\omega_H + \omega_C) - J(\omega_H - \omega_C)}{J(\omega_H - \omega_C) + 3J(\omega_C) + 6J(\omega_H + \omega_C)}\right] \quad (2)$$

In these expressions, ω_H and ω_C are the Larmor frequencies of ^{1}H and ^{13}C nuclei, respectively (with units of rad/s), n is the number of protons attached to the ^{13}C nuclei of interest (n = 2 for methylene carbons), γ_H and γ_C are the gyromagnetic ratios of ^{1}H and ^{13}C, and K is a constant which depends on the average C−H internuclear distance (equal to 2.29×10^9 s^{-2} here[46]).

For deuterium nuclei, spin−lattice relaxation is dominated by electric quadrupole coupling and has the following relationship to the reorientation of a C−D bond:[43−45]

$$\frac{1}{T_1} = \frac{3}{10}\pi^2\left(\frac{e^2qQ}{h}\right)^2[J(\omega_D) + 4J(2\omega_D)] \quad (3)$$

Here ω_D is the Larmor frequency of deuterium. The deuterium quadrupole coupling constant e^2qQ/h was taken as 172 kHz for the backbone deuterons.[44,47]

In the three equations above, $J(\omega)$ is the spectral density function:

$$J(\omega) = {}^1/_2\int_{-\infty}^{\infty} G(t)\exp(-i\omega t)\,dt \quad (4)$$

Here $G(t)$ is the orientation autocorrelation function which describes the reorientation of the internuclear vector (^{13}C−H or C−D bonds in our experiments):

$$G(t) = \frac{3}{2}\langle\cos^2\theta(t)\rangle - \frac{1}{2} \quad (5)$$

Here $\theta(t)$ is the angle of a ^{13}C−H or C−D bond at time t relative to its original position. The brackets denote the ensemble average over a collection of bond vectors.

The modified Kohlrausch−Williams−Watts (mKWW) function has been shown to give an excellent representation of the autocorrelation function in previous studies[39,48−50] and is used here:

$$G(t) = a_{lib}\exp\left(-\frac{t}{\tau_{lib}}\right) + (1 - a_{lib})\exp\left[-\left(\frac{t}{\tau_{seg}}\right)^{\beta}\right] \quad (6)$$

Here a_{lib} and τ_{lib} characterize the amplitude and relaxation time for the librational motion. Fits to the experimental data were insensitive to τ_{lib}, and this parameter was set equal to 1 ps. τ_{seg} and β describe a characteristic segmental relaxation time and its distribution. We assume that τ_{seg} follows a Vogel−Tammann−Fulcher (VTF) temperature dependence.[51] The VTF equation is equivalent to the Williams−Landel−Ferry (WLF) equation and is given by[52]

$$\log\left(\frac{\tau_{seg}}{\tau_\infty}\right) = \frac{B}{T - T_0} \quad (7)$$

where τ_∞, B, and T_0 are constants for a given component in a particular sample. The segmental correlation time $\tau_{seg,c}$ is defined as the integral of the segmental portion of the correlation function:

$$\tau_{seg,c} = \frac{\tau_{seg}}{\beta}\Gamma\left(\frac{1}{\beta}\right) \quad (8)$$

PGSE NMR Diffusion Measurements. PGSE diffusion experiments in the proton resonance, aided by transverse relaxation measurements, were carried out on a 33 MHz spin-lock CPS-2 spectrometer operating with a wide-gap electromagnet. Gradient coils supplied horizontal gradients of calibrated magnitudes decreasing from G = 710 to 573 G/cm as the temperature was raised between 30 and 110 °C and from G = 243 to 210 G/cm as temperature was increased between 130 and 192 °C. The temperature is controlled to within ±0.2 °C of the set point by the flow of heated air through the NMR-PGSE probe. Principal-echo transverse magnetization decays were nonexponential but unimodal, with T_2 ranging between 12 and 50 ms.

The nonspectroscopic PGSE experiments were performed at fixed G by varying the duration δ of each of the pair of gradient pulses coordinated with the stimulated-echo rf pulse sequence. In this work the rf pulse spacing τ between the first two 90° pulses was 18 ms, and the spacing between the first and third pulses, hence also the spacing Δ between the gradient pulses, was 100 ms. To minimize residual gradient

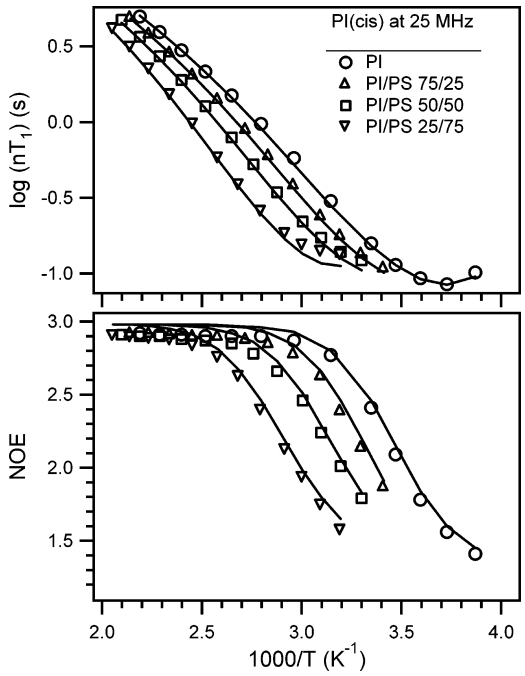

Figure 2. ^{13}C T_1 and NOE for C1 carbon of *cis*-PI as a homopolymer and in three PI/PS blends at 25.1 MHz. The solid curves are fits using the mKWW autocorrelation function and VTF temperature dependence. The fit parameters are listed in Table 2.

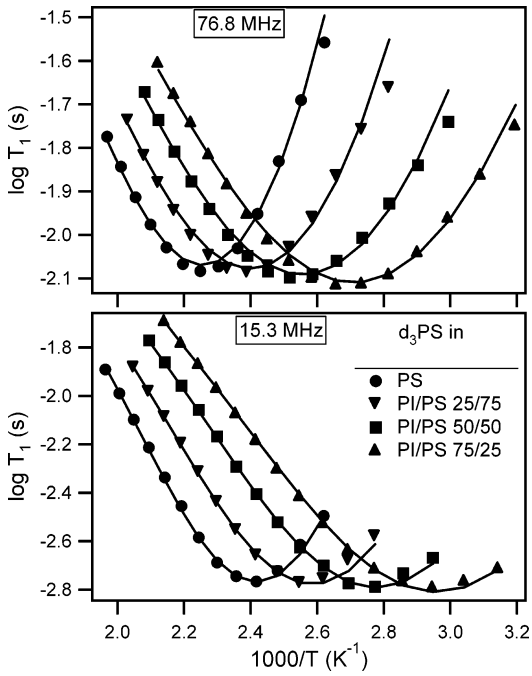

Figure 3. ^{2}H T_1 for backbone deuterons of PS as a homopolymer and in three PI/PS blends at 76.8 and 15.3 MHz. The solid curves are fits using the mKWW autocorrelation function and VTF temperature dependence. The fit parameters are listed in Table 2.

effects, Δ was never larger than $\delta - 6$ ms but usually did not exceed 3 ms. A steady gradient $G_0 = 0.35$ G/cm parallel to G was used for convenience in data collection. Between 8 and 12 values of δ were employed to produce a maximal echo attenuation to below 3% of the original echo. Signal averaging of between 5 and 20 passes for each δ improved the signal-to-noise ratio. Experiments were conducted off-resonance by -3 kHz in single-sideband mode with single-phase rf phase-sensitive detection, and the echo signal A was measured as the integral over the magnitude Fourier transform of the beat between echo and reference, after correction for rms baseline noise. Several independent checks revealed no explicit dependence of the extracted diffusion coefficient on δ, ensuring that the diffusion was Fickian.

Data reduction was performed off-line by the current PC version of a Fortran program[53] which accounts for residual gradient effects,[54] known polymer polydispersity,[55] and multicomponent diffusion.[55,56] The measured echo attenuation curves reflected a modest, smooth D distribution:

$$\frac{A(X)}{A(0)} = \sum_i^N w_i \exp\left(-\frac{\tau_1}{T_{2i}}\right) \exp(-\gamma_H{}^2 D_i X) \qquad (9)$$

where $X = (G\delta)^2(\Delta - \delta/3)$ with small additional terms in GG_0; γ_H denotes the proton gyromagnetic ratio. The normalized sum over $N = 10$ terms simulated a log−normal distribution by coordinating weights w_i with corresponding diffusivities D_i. The two fitted parameters were a mean diffusivity $\langle D \rangle$ and a standard deviation σ_D. The latter never exceeded 20% of $\langle D \rangle$, as expected for modest molecular weight dispersity. The estimated weak dependence of T_2 on molecular weight in the ensemble was also routinely included in the fitted model. The resulting fits were successful in all cases.

III. Results and Discussion for Segmental Dynamics

***T*$_1$ and NOE Data.** Figures 1 and 2 show the ^{13}C T_1 and NOE data for the C1 methylene carbon of *cis*-PI as a homopolymer and in three PI/d_3PS blends, measured at two magnetic fields. The T_1 minimum moves to higher temperature as the fraction of the d_3PS component increases. Since the T_1 minimum approximately indicates the temperature at which the segmental dynamics occur on a 1 ns time scale, this indicates that the segmental dynamics of PI chains are slowed by the surrounding d_3PS chains. Qualitatively, this is consistent with the higher T_g of d_3PS relative to PI. The NOE data exhibit the same variation with composition, shifting to higher temperature with increasing d_3PS fraction.

Figure 3 shows the ^{2}H T_1 data for the backbone deuterons of d_3PS as a homopolymer and in three PI/d_3PS blends, measured at two magnetic fields. The T_1 minimum moves toward lower temperature with increasing PI content, qualitatively indicating that the segmental dynamics of d_3PS chains become faster due to the presence of surrounding PI chains.

Fits to the mKWW and VTF Functions. Although the variation of T_1 minimum with blend composition qualitatively indicates the effect of mixing on the component segmental dynamics, fitting the experimental data to a model correlation function allows us to extract the segmental correlation times and have a quantitative description of the experimental results. Since it was found in previous studies[39,48−50] that the mKWW function (eq 6) provides excellent fits to the NMR relaxation data, we employed it here in combination with the assumption of a VTF temperature dependence (eq 7) for the segmental relaxation times.

For each component in each sample, fitting was performed on T_1 (and NOE) values at two fields simultaneously using eqs 1−7. The NMR experiments do not directly measure the orientation autocorrelation function $G(t)$. In our fitting, we make an initial guess about the fit parameters, calculate the resulting T_1 and NOE, and then optimize the parameters to provide the best

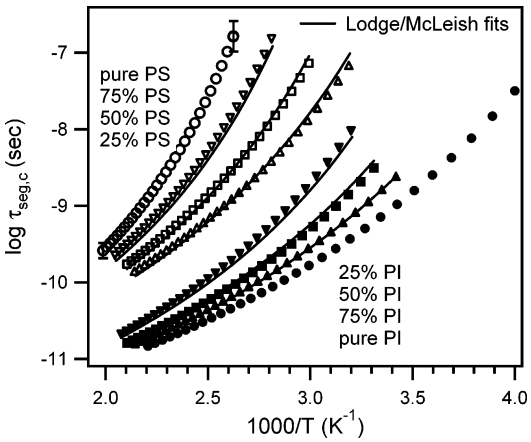

Figure 4. Segmental correlation times (calculated from the fit parameters in Table 2 and shown as symbols) for PI and PS as homopolymers and in three PI/PS blends. Representative error bars are shown and reflect the uncertainty associated with the fitting procedure. The solid lines are fits to the Lodge/McLeish model with $\phi_{self}(PI) = 0.33$ and $\phi_{self}(PS) = 0.42$.

Table 2. Fit Parameters for Segmental Dynamics of PI and d_3PS in Homopolymers and Blends

	fit parameters	pure PI	PI/d_3PS 75/25	PI/d_3PS 50/50	PI/d_3PS 25/75	pure d_3PS
PI	τ_∞ (ps)	0.25	0.25	0.21	0.14	
	T_0 (K)	152	166	180	199	
	B (K)	484	476	476	502	
	β	0.62	0.58	0.52	0.46	
	a_{lib}	0.41	0.42	0.42	0.44	
d_3PS	τ_∞ (ps)		0.55	0.55	0.47	0.44
	T_0 (K)		194	216	245	273
	B (K)		569	569	569	569
	β		0.50	0.50	0.49	0.51
	a_{lib}		0.13	0.17	0.17	0.21

fit to the NMR data. There are five unknown parameters in this procedure: a_{lib}, β, τ_∞, B, and T_0. The fit parameters are summarized in Table 2 and yield satisfactory fits to the experimental data. The fits are shown in Figures 1−3 by the solid lines. The slight mismatch at high NOE values in Figure 2 is due to the absence of long time relaxation in the mKWW equation (eq 6) and does not indicate a failure to accurately describe the segmental dynamics.[49,50] When fitting the data for the d_3PS component in the blends, B was constrained to 569 K (the value obtained from fitting T_1 data for the d_3PS homopolymer). The uncertainty in segmental correlation times introduced by this constraint is less than 0.1 decade. Because of the relatively small range of correlation times probed by NMR experiments, B and T_0, and a_{lib} and β, are highly correlated with each other in our fitting procedure. This leads to substantial uncertainties in those parameters: B is accurate within ±100 K, T_0 is accurate within ±15 K, and both a_{lib} and β have an uncertainty of ±0.1.

Segmental Correlation Times. The segmental correlation times $\tau_{seg,c}$ of PI and d_3PS in the homopolymers and three blends were calculated from the fit parameters in Table 2 and are presented in Figure 4 as the symbols. As expected from the homopoloymer T_gs and consistent with the trends of T_1 minimum variation, $\tau_{seg,c}$ of the PI component at a given temperature increases as the d_3PS fraction increases. On the other hand, $\tau_{seg,c}$ of the d_3PS component at a given temperature decreases as the PI fraction increases in the blends. These effects are more pronounced at lower temperatures. Qualitatively, the segmental dynamics of the PI and d_3PS components in the blends are modified to some extent by blending but still remain distinct. The uncertainty in the reported $\tau_{seg,c}$ values, as reflected by different fitting procedures and variations of the fit parameters, is shown by the representative error bars in Figure 4.

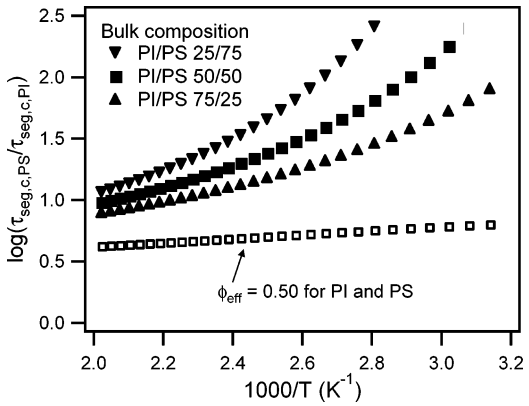

Figure 5. Ratios of segmental correlation times of PS and PI in the PI/PS blends. The solid symbols are ratios in particular blends. In any given blend, the two components have distinct segmental dynamics with independent temperature dependences. The open symbols are ratios of correlations times at the same effective composition (0.50) based on the Lodge/McLeish model. Within the context of the model, the open symbols indicate the intrinsic mobility difference of the PI and PS chains due to the difference in their chemical structure.

The solid symbols in Figure 5 show the ratio of segmental correlation times of d_3PS and PI in the blends versus temperature. For any sample at a given temperature, the segmental dynamics of the d_3PS component are always slower than that of the PI component. The ratio of segmental correlation times grows larger as the temperature is lowered and as the PS fraction in the blend increases. We ascribe this local dynamic heterogeneity to the large dynamic difference between PI and d_3PS homopolymers ($\Delta T_g = 130$ K).

Lodge/McLeish Model. The Lodge/McLeish model provides a framework for interpreting and predicting the component dynamics in miscible polymer mixtures.[30] It assumes that the segmental relaxation process of a given segment in a polymer mixture is affected by the local composition in a surrounding region with a length scale of the Kuhn segment l_k. The effective local concentration ϕ_{eff} is given by

$$\phi_{eff} = \phi_{self} + (1 - \phi_{self})\phi \tag{10}$$

Here ϕ_{self} is the self-concentration of the polymer under consideration. It is determined from the volume fraction occupied by one Kuhn length of the polymer inside a volume $V = l_k^3$:

$$\phi_{self} = \frac{C_\infty M_0}{k\rho N_{av} V} \tag{11}$$

Here M_0 is the molar mass of the repeat unit, N_{av} is the Avogadro constant, k is the number of backbone bonds per repeat unit, ρ is the bulk density, and C_∞ is the characteristic ratio.

The model associates the average local concentration ϕ_{eff} for each component with a local glass transition

temperature $T_{g,eff}(\phi) = T_g(\phi_{eff})$, which is assumed to obey the Fox equation:[11]

$$\frac{1}{T_g(\phi_{eff})} = \frac{\phi_{eff}}{T_g^A} + \frac{1-\phi_{eff}}{T_g^B} \quad (12)$$

The component dynamics in the mixtures can be predicted by correlating the changes in $T_{g,eff}$ with the changes in T_0

$$T_{0,i}(\phi) = T_{0,i} + [T^i_{g,eff}(\phi) - T^i_g] \quad (13)$$

and by assuming that the remaining VTF parameters (B, τ_∞) do not change with mixing.[11] Here "i" denotes component A or B.

Comparison to the Lodge/McLeish Model. The Lodge/McLeish model successfully fits the segmental correlation times of both components in PI/d_3PS blends with $\phi_{self}(PI) = 0.33 \pm 0.05$ and $\phi_{self}(d_3PS) = 0.42 \pm 0.07$. The fits are shown in Figure 4 by the solid lines. The only input information in the fitting procedure is the segmental dynamics of the homopolymers; we treat ϕ_{self} as an adjustable parameter. For each component, the ϕ_{self} value and the $\tau_{seg,c}$ curve of the homopolymer generate the three fitting curves. The uncertainty in the fitted ϕ_{self} is estimated by the point where the deviation from the fitting is comparable to the experimental uncertainty. The fits nicely reflect the variation in the segmental dynamics of both PI and d_3PS components with the composition and temperature.

In a recent paper, we used the Lodge/McLeish model to interpret the segmental dynamics of SISI tetrablock copolymers.[32,42] The values obtained for ϕ_{self} for styrene and isoprene segments in that paper are different than those reported here. In the framework of the Lodge/McLeish model, it is expected that the ϕ_{self} values should be the same for styrene and isoprene units in the miscible polymer blends and disordered block copolymers. Here is an explanation for this discrepancy. In the Lodge/McLeish model, the homopolymer T_gs are two critical inputs. In the case of polymer blends, these are straightforward to measure. For the SISI tetrablock copolymers, the samples were nearly equal in total degree of polymerization (N), but the relative block lengths of the styrene and isoprene segments (N_S and N_I) varied with composition. In our previous work, we used T_g values for PS and PI homopolymers with the similar total degree of polymerization N as inputs. We now realize that it is more appropriate to use T_g values for PS and PI homopolymers corresponding to the block length (N_S and N_I) for each SISI tetrablock sample. We reanalyzed the SISI data in this way and obtained good fits to the data. Values of $\phi_{self}(PI) = 0.34 \pm 0.07$ and $\phi_{self}(PS) = 0.40 \pm 0.10$ were obtained, which are consistent with the fit parameters reported here for PI/PS blends. The fits obtained in this manner are as good as those shown in our published work.[32] In our revised analysis of the SISI data, the homopolymer T_gs were estimated from reported empirical relationships between molecular weight and glass transition temperature.[57] The junction effect was taken into account in this fitting procedure.[58]

The Lodge/McLeish model (eq 11) predicts values of $\phi_{self}(PI) = 0.45$ and $\phi_{self}(PS) = 0.27$. The difference between the predicted and fitted values is beyond experimental uncertainty. As pointed out by Lodge and McLeish,[30] a factor of order unity may be missing from eq 11, since the choice of $V = l_k^3$ is somewhat arbitrary. For example, a spherical or cylindrical volume could be chosen instead of a cube. One way to discuss the differences between the predicted and observed ϕ_{self} values is to calculate the corresponding length scales.[59] Equation 11 assumes that composition on the scale of l_k controls dynamics. For PS, $l_k = 1.5$ nm. If we assume that the rest of the fitting equations are correct, we can infer from the fitted value of ϕ_{self} that the actual length scale relevant for segmental dynamics is 1.2 nm. While other assumptions made in fitting the data may not be valid, this calculation does show that only a small adjustment in length scale is needed to bring eq 11 and the experimental results into agreement. In a recent study, the segmental dynamics of isolated PI chains in host matrices of PB, PVE, and PS were investigated.[60] The fitted ϕ_{self}(PI) values vary among the matrices. Within the framework of the Lodge/McLeish model, this indicates that the relevant local volume depends on blending partner.

Molecular dynamics simulations have been performed on the PI/PS blend system (same molecular weights as in these experiments) to provide an atomistic view of the effect of blending on structure and dynamics.[61] This work shows a strong correlation between local dynamics and local composition, in qualitative accord with the Lodge/McLeish model. Reference 61 reports that local composition at distances of up to 1.3 nm from a given segment influence segmental dynamics, in good qualitative agreement with the length scales inferred from fitting to the Lodge/McLeish model.

Intrinsic Mobility Difference. In our implementation of the Lodge/McLeish model, the dynamic disparity of the PI and PS components in a given blend (solid symbols in Figure 5) is a result of two factors: (1) the different effective local compositions experienced by each component; (2) the different dynamics of the two homopolymer melts. Within the context of the model, we can separate these two contributions by comparing the dynamics of the PI and PS segments at equal effective compositions instead of equal bulk compositions.

The open symbols in Figure 5 represent the ratio of segmental correlation times of the PI and PS segments in local environments with an effective composition of 0.50. This ratio is nearly independent of composition (not shown) and should be attributed to the different intrinsic mobility of the two kinds of chains. The intrinsic mobility difference of the PI and PS chains originates from the differences in their molecular structure and intermolecular potentials. The segmental correlation times of the PI and PS segments at a given effective composition were calculated from the Lodge/McLeish model using $\phi_{self}(PI) = 0.33$ and $\phi_{self}(PS) = 0.42$.

Similar Dynamics of *cis*- and *trans*-PI Units. ^{13}C T_1 and NOE values for the C1 methylene carbon of *trans*-PI units in the PI homopolymer and in three PI/d_3PS blends were also measured at two magnetic fields. They are slightly different than the corresponding values for *cis*-PI units. The T_1 and NOE values for *trans*-PI units can be found in the Supporting Information (Figures S1 and S2).

For the PI homopolymer, the segmental correlation times of *trans*-PI units were extracted by fitting the T_1 and NOE data and following the same fitting procedure as we did for *cis*-PI units (eqs 1−7). In the temperature range of study, *cis*-PI and *trans*-PI units have identical

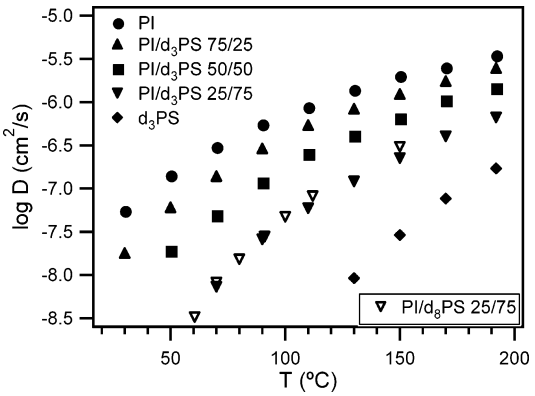

Figure 6. Diffusion coefficients measured by PGSE NMR diffusion experiments. The filled symbols represent average diffusion coefficients (D) of the two components in PI/d_3PS blends; the open symbols represent diffusion coefficients of the PI component (D_{PI}) in the PI/d_8PS 25/75 blend. Within experimental error, the filled and open symbols for the 25/75 blend are identical. This and other evidence (see text) indicates that the PI and PS components have essentially identical diffusion coefficients in these blends.

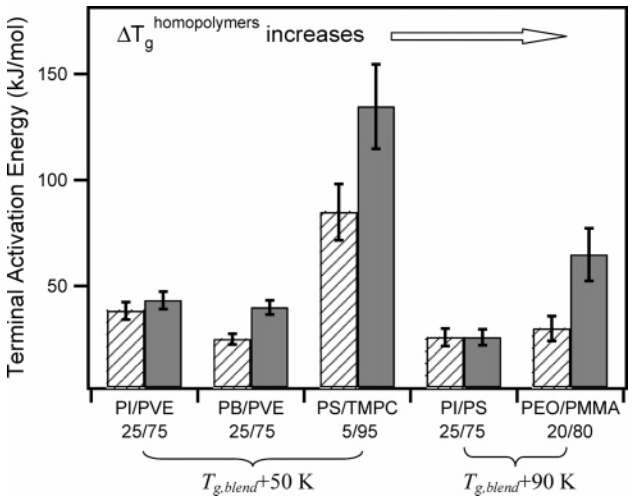

Figure 7. Activation energy of terminal dynamics for five miscible polymer blends at selected temperatures and compositions. For each blend, the left and right bars correspond to lower and higher T_g components, respectively. Error bars represent our estimates based upon the uncertainty of the reported data. PI/PS is an unusual blend in that the terminal dynamics of the two components show unexpected identical temperature dependences.

segmental dynamics within 0.05 decade. (The results are presented in Figure S3 of the Supporting Information.) In contrast, a previous study reported that in a polybutadiene (PB) homopolymer the cis units have a stronger temperature dependence than the trans units over a similar temperature regime.[26] Given the similarity of PI and PB in terms of structures and T_g values, this is a surprising contrast. We speculate that the chemical difference between PI and PB (a methyl group) plays a critical role. We expect that the side groups in PI enhance the dynamic coupling between cis and trans units on different chains. Because of the structural difference, less coupling presumably occurs in PB.

In the three blends, the segmental dynamics of *trans*-PI units exhibit the same composition dependence as that of *cis*-PI units. The composition dependence was determined by shifting the T_1 and NOE data of the PI component in the blends to those of the PI homopolymer. The same temperature shifts sufficed to superpose the T_1 and NOE data for both *cis*- and *trans*-PI units, and the resulting superpositions are of the same quality.

IV. Results and Discussion for Diffusion

Diffusion Coefficients. PGSE NMR diffusion measurements were made on six samples: five PI/d_3PS samples (100/0, 75/25, 50/50, 25/75, 0/100) and one PI/d_8PS blend (25/75). The resulting diffusion coefficients are presented in Figure 6. PGSE NMR diffusion experiments were performed by transverse relaxation measurements in proton resonance. For the PI/ d_3PS blends, there are eight protons on each PI unit and five protons on each d_3PS unit. Thus, in principle, the echo attenuation curves will be bimodal, reflecting the motion of both PI and d_3PS components in the blends. If the diffusion coefficients of the two components in a binary system differ by more that a factor of 3, a continuous unimodal distribution of D (eq 9) will fail to fit the measured attenuation curves; in such cases the bimodality will be clearly evident and demand a fit of a superposition of two distinct components corresponding to the two values of D. All the echo attenuation curves in our experiments are well fit by a unimodal distribution of D. Thus, we conclude that the diffusion coefficients of PI and d_3PS components (D_{PI} and D_{PS}) in the blends are identical within a factor of 3 and that both are near the reported average D values in Figure 6.

Measurements on PI/d_8PS 25/75 were performed to verify the conclusion that $D_{PI} \approx D_{PS}$. In this case only D_{PI} is measured due to the perdeuteration of the d_8PS component. Figure 6 shows that D_{PI} completely tracks the average D value obtained from measurements on the PI/d_3PS (within 0.1 decade). Since the latter are dominated by the PS component, this confirms our conclusion that the two components in PI/PS blends have essentially identical diffusion coefficients, as reported by the D values in Figure 6. Since both chains are nearly equal in length (13 units for PI and 15 units for PS), this means their monomeric friction coefficients ζ are also essentially identical according to the Rouse model:

$$\zeta = \frac{kT}{ND} \tag{14}$$

Here k is the Boltzmann constant and N is the degree of polymerization.

Diffusion in PI/PS Blends Is Unusual. It is a striking result that PI and PS chains have identical monomeric friction coefficients in their blends, considering the significant structural and dynamic disparity ($\Delta T_g = 130$ K) and the distinct segmental dynamics in these blends. To put this observation in context, we compare PI/PS with other miscible blend systems in this section.

The terminal dynamics in PI/PVE,[11] PB/PVE,[21] PS/TMPC,[19] PS/PXE,[18] and PEO/PMMA[2] have been investigated by either rheology or diffusion experiments. For each blend, the monomeric friction coefficients ζ of the two components were separately extracted. In Figure 7, we compare the temperature dependences of ζ (apparent activation energies) for the two components. In constructing this figure, we chose to compare blends that contained more high T_g polymer than low T_g polymer and to make the comparison at lowest temperatures for which data are available, as these tend to be the conditions under which the two activation energies

are the most different. The selection of temperature and composition does not affect the qualitative features of the figure.

In Figure 7, we have arranged the blends so that the T_g differences of the two homopolymers ($\Delta T_g^{\text{homopolymers}}$) increase from left to right. In PB/PVE, PS/TMPC, and PEO/PMMA, the terminal activation energies of the two components are different beyond experimental uncertainty.[62] For PI/PVE, the difference is not significant, and we ascribe this to the relatively small difference in the homopolymer T_gs (~60 K). This explanation is supported by the trend that the relative activation energy difference of the two components in these four blends becomes larger with increasing $\Delta T_g^{\text{homopolymers}}$. Given this trend, it is quite unexpected that the temperature dependences of terminal dynamics for the two components in PI/PS blends are so similar.

There is one other miscible blend system with a large ΔT_g in which the two components are known to have similar activation energies for terminal dynamics: PS/PXE (55/45).[18] In this case, the similarity in terminal dynamics is likely due to the essentially identical component segmental dynamics.[17]

Why Do the Two Components in PI/PS Blends Have Identical Terminal Dynamics? Given the fact that the segmental dynamics of the two components in PI/PS differ by orders of magnitude and also have significantly different temperature dependences (Figure 5), it is quite striking that PI and PS components in PI/PS blends have identical terminal dynamics.

Drawing on ideas in the literature,[32,63,64] we speculate that thermodynamic barriers play a critical role in controlling the terminal dynamics in PI/PS blends. Of the six blends discussed above, PI/PVE, PS/TMPC, PEO/PMMA, and PS/PXE[65] have negative χN; PB/PVE has a small positive χN ($\approx$0.03); only PI/PS has large positive χN ($\approx$1.5).[66] The critical temperature for phase separation for the PI/PS blends is just below the lowest temperatures of our measurements. We imagine that the unfavorable interaction between PI and PS components poses a significant thermodynamic barrier to the diffusion of PI (or PS) chains across PS (or PI) rich environments. If these barriers are sufficiently high, then all the chains will be trapped in free energy minima (environments enriched in same type of chains) until fluctuations in the blend matrix allow them to move to a neighboring region. In this scenario, all chains are slaved to the collective dynamics of the blend matrix. This would account for the essentially identical diffusion coefficients of the PI and PS components in their blends. In this scenario, there should be no influence from χ on the segmental dynamics. This is because the Kuhn length is comparable to or smaller than the correlation length in these PI/PS blends.[67] Thus, on the length scale relevant for segmental dynamics, the average local composition around a given segment is the same as it would be if χ were equal to zero. In summary, thermodynamic barriers in PI/PS blends could have a profound influence on terminal dynamics without influencing the segmental dynamics.

The idea that thermodynamic fluctuations in polymer blends influence the diffusion of the components has been previously explored by Tang and Schweizer.[63] They predict suppression of diffusion in fluctuating polymer blends above but near the critical points. Direct quantitative comparison with the results for diffusion in PI/PS blends is complicated due to the very large asymmetry in homopolymer friction coefficients, which is not accounted for in the theory. However, by assuming a dynamically symmetric blend with similar molecular weights and χ as the PI/PS blends here, the theory predicts a suppression of diffusion of about a factor of 2. In our experiments, the diffusion of the fast component PI is more than 1 decade slower than what we would predict by assuming that segmental dynamics are the only dominant driving force for the terminal dynamics.

There are additional precedents for invoking thermodynamics to explain homogeneous terminal diffusion. Milhaupt et al. investigated the monomeric friction coefficients ζ of PI and PS tracers diffusing in disordered styrene−isoprene tetrablock copolymers (SISI).[64] They found that, for a given matrix, ζ_{PI} and ζ_{PS} are essentially equivalent. This is striking given that the segmental dynamics of the styrene and isoprene segments in SISI chains differ by orders of magnitude.[42,68] The homogeneous tracer diffusion in SISI was attributed to coupled diffusion, induced by thermodynamic barriers.[32,64] The static structure factor $S(q)$ for the disordered SISI copolymers contains a peak associated with the block structure.[36] Qualitatively, this peak signifies a segregation of styrene and isoprene units on the length scale of the radius of gyration that could pose a significant thermodynamic barrier to tracer diffusion. While PI/PS blends are similar to SISI block copolymers in many respects, there is an important structural difference that creates uncertainty about extending this explanation to the PI/PS blends. Concentration fluctuations in miscible blends are qualitatively different than those in disordered block copolymers. In particular, $S(q)$ for miscible PI/PS blends does not show a peak at length scales corresponding to the chain dimensions.[67] So even if the "thermodynamic barrier" explanation for homogeneous diffusion is correct for SISI block copolymers, it does not necessarily need to be correct for PI/PS blends.

An alternate origin for homogeneous terminal diffusion in PI/PS blends might be associated with the low molecular weights of the PI and PS chains used in this study. In Figure 7, the PI/PS blend is the only system for which both components are short chains. While it is clear that extremely short chains would have homogeneous terminal dynamics, at present we do not have a mechanism which would allow homogeneous terminal diffusion to emerge in a molecular weight regime where the chains are long enough for the component segmental dynamics to be strongly heterogeneous.

The above explanations for homogeneous terminal diffusion in PI/PS blends could be tested in a number of ways. One idea is to change the molecular weight of one component in PI/PS blends to see whether the two components still have identical diffusion coefficients. Neutron scattering experiments are being performed to characterize the concentration fluctuations in this system.

Mixing Rule Predictions. As discussed above (Figure 6), PI and PS chains have essentially the same diffusion coefficients in their blends and very similar monomeric friction coefficients ζ, since both types of chains are nearly equal in length (13 units for PI and 15 units for PS). We have averaged this small difference and plotted the average ζ in Figure 8 (calculated from eq 14 by setting $N = 14$).

We now explore two possible ways to understand the average terminal dynamics (ζ) of miscible polymer

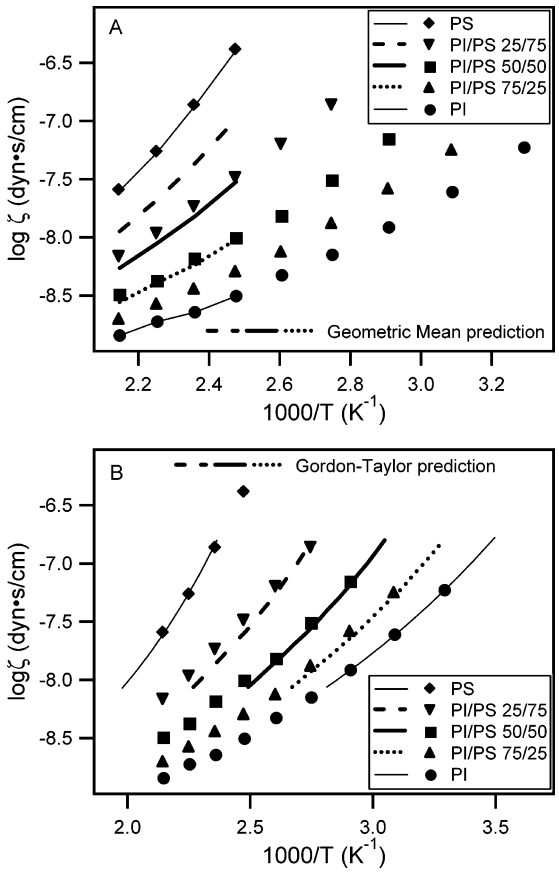

Figure 8. Monomeric friction coefficients ζ for PI/PS blends compared with two mixing rule predictions: (A) geometric mean (eq 15); (B) Gordon−Taylor equation (eq 16). ζ was calculated from the diffusion coefficients D in Figure 6 using eq 14. While the geometric mean prediction significantly overestimates ζ, the Gordon−Taylor prediction provides a nearly quantitative description.

blends from the homopolymer values (ζ_A^0 and ζ_B^0). A variety of semiempirical mixing rules have been proposed previously. In these approaches, the component dynamics are averaged in some manner at each temperature. The simplest mixing rule of this type is the volume fraction weighted geometric mean:[69]

$$\log \zeta(\phi) = \phi \log \zeta_A^0 + (1 - \phi) \log \zeta_B^0 \qquad (15)$$

where ϕ is the volume fraction of component A. In this approach, the dynamics of the two components are averaged at a given temperature.

A second type of mixing rule averages the temperatures at which dynamics occur at a given rate. Here we use the Gordon−Taylor equation[70]

$$T_\zeta(w) = \frac{wT_{\zeta,A} + k(1 - w)T_{\zeta,B}}{w + k(1 - w)} \qquad (16)$$

where w is the weight fraction of component A and k is an adjustable parameter. Usually the Gordon−Taylor equation is applied to T_g values. Here we generalize this procedure and apply it for each value of ζ (we denote the temperature associated with a particular friction coefficient as T_ζ). Both T_g and T_ζ are temperatures at which dynamics occur at a particular rate.

The predictions based on the two methods described above are presented in parts A and B of Figure 8 as the three thick lines, corresponding to the three blend compositions. While the geometric mean mixing rule significantly overestimates the friction experienced by PI and PS segments in the blends, the Gordon−Taylor mixing rule closely follows the data points.

A few details about the construction of Figure 8B need to be specified. Ideally, the adjustable parameter k should be determined by fitting the T_g values of PI/PS blends. Since we cannot measure the T_gs of the PI/PS blends due to phase separation, the k parameter was determined from disordered styrene−isoprene tetrablock copolymers,[36] and the resulting value of $k = 2.0$ was used in our prediction. We chose the Gordon−Taylor equation instead of the Fox equation since the latter gives an unsatisfactory description of the T_g data. We also predicted the average monomeric frictions using the Fox equation, and the resulting predictions (not shown here) are somewhat worse than Figure 8B but much better than the geometric mean predictions. In using eq 16, we extended the temperature range of homopolymer data slightly in order to predict as many blend results as possible.[71]

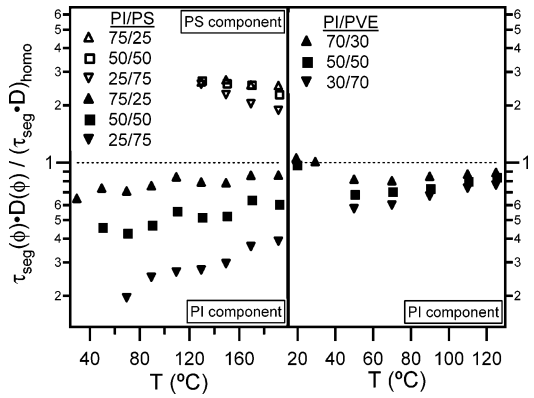

Figure 9. Comparison of the temperature and composition dependences of terminal and segmental dynamics for PI and PS components in PI/PVE and PI/PS blends. The vertical axis scales $\tau_{seg}D$ of a component in blends to its value for the homopolymer. The terminal dynamics of both components in PI/PS blends do not follow the temperature and composition dependences of their segmental dynamics, while the terminal dynamics of PI in PI/PVE exhibit temperature and composition dependences that are very similar to those of the PI segmental dynamics.

Comparison of Segmental and Terminal Dynamics. Having measured the segmental and terminal dynamics for both components in PI/PS blends, we are able to compare the temperature and composition dependences for each component. The terminal dynamics are characterized by diffusion coefficients D in this study. The left side of Figure 9 plots $\tau_{seg}(\phi)D(\phi)$ over the temperature range of study for PI and PS in the three PI/PS blends. The vertical axis scales $\tau_{seg}(\phi)D(\phi)$ of each component in blend to its homopolymer value. $\tau_{seg}D$ is independent of temperature for the two homopolymers in our study (±15%) and for most homopolymer melts at temperatures considerably above T_g.[37−39] Thus, in Figure 9, any slope other than zero reflects a different temperature dependence for segmental and terminal dynamics, and any deviation from the center flat line reflects a different composition dependence for segmental and terminal dynamics. The left side of Figure 9 shows that, for PI in PI/PS blends, the terminal dynamics have stronger temperature and composition dependences than the segmental dynamics; for PS in PI/PS blends, the terminal dynamics have weaker tempera-

ture dependence and stronger composition dependence than the segmental dynamics.

In a previous study, similar segmental dynamics and diffusion measurements were performed on the PI component in PI/PVE blends.[11] These data are presented on the right side of Figure 9 to allow a clear comparison between the PI/PS and PI/PVE systems. All the points for PI in PI/PVE blends are much closer to the center flat line with the deviation comparable to the experimental uncertainty (about a factor of 2). This is consistent with the conclusion that, in PI/PVE blends, the segmental and terminal dynamics exhibit equivalent dependences on temperature and composition.[11] As discussed above, we attribute the difference between PI/PVE and PI/PS to the presence of thermodynamic barriers to diffusion in the PI/PS system.

V. Conclusions

In this work we investigated the segmental and terminal dynamics of both components in PI/PS blends by using isotopic labeling and the selectivity of NMR. Though this system has a large positive thermodynamic interaction parameter $\chi \sim 0.1$, it is miscible in the temperature range of our study due to low molecular weight. ^{13}C and ^{2}H NMR relaxation time measurements were performed over a wide range of temperatures and compositions to extract the segmental correlation times. Pulse-gradient spin-echo NMR was used to determine the diffusion coefficients. Diffusion measurements were taken on the same set of samples over a similar temperature window as the segmental dynamics measurements. The combined results allow us to further test the Lodge/McLeish model and probe the molecular origin of segmental and terminal dynamics in miscible polymer blends. Our principal conclusions are as follows:

(1) The two components in PI/PS blends exhibit distinct segmental dynamics as expected. The dynamic difference between PI and PS components ranges from 1 decade at 500 K to more than 2 decades at $T_g^{blend} + 50$ K. Quantitatively, the results are well described by the Lodge/McLeish model. The fit parameters ϕ_{self} are somewhat different than the model predictions.

(2) Surprisingly, the PI and PS chains in these blends have essentially identical terminal dynamics (either characterized by diffusion coefficients D or monomeric friction coefficients ζ). We know of no other system with distinct segmental dynamics and large ΔT_g showing this behavior. This observation can be understood if thermodynamic barriers to diffusion in this system are so substantial that all chains are slaved to the collective dynamics of the blend matrix. The average terminal dynamics are well reproduced by the Gordon−Taylor mixing rule.

(3) *Cis* and *trans* segments in the PI homopolymer have identical segmental dynamics over the temperature range of study, while in a polybutadiene homopolymer, the cis units have a stronger temperature dependence than the trans units. We speculate that the absence of side groups in PB explains this.

Acknowledgment. This work is supported by the National Science Foundation (DMR-0355470). We thank Tim Lodge and Ralph Colby for helpful discussions and thank Paul Nealey for the use of the DSC. Some measurements were performed at the Instrument Center of the Department of Chemistry, University of Wisconsin−Madison, supported by NSF CHE-9629688.

Supporting Information Available: Figures S1 and S2 present ^{13}C T_1 and NOE data for the trans units of PI as a homopolymer and in three PI/PS blends at 125.8 and 25.1 MHz; Figure S3 presents the segmental correlation times of the cis and trans units in the PI homopolymer; the *cis* and *trans* geometric isomers exhibit identical segmental dynamics within experimental error. This material is available free of charge via the Internet at http://pubs.acs.org.

References and Notes

(1) Minnick, M. G.; Schrag, J. L. *Macromolecules* **1980**, *13*, 1690−1695.
(2) Colby, R. H. *Polymer* **1989**, *30*, 1275−1278.
(3) Roovers, J.; Toporowski, P. M. *Macromolecules* **1992**, *25*, 1096−1102.
(4) Pathak, J. A.; Colby, R. H.; Floudas, G.; Jerome, R. *Macromolecules* **1999**, *32*, 2553−2561.
(5) Chung, G. C.; Kornfield, J. A.; Smith, S. D. *Macromolecules* **1994**, *27*, 5729−5741.
(6) Alegria, A.; Colmenero, J.; Ngai, K. L.; Roland, C. M. *Macromolecules* **1994**, *27*, 4486-4492.
(7) Zawada, J. A.; Fuller, G. G.; Colby, R. H.; Fetters, L. J.; Roovers, J. *Macromolecules* **1994**, *27*, 6861−6870.
(8) Adams, S.; Adolf, D. B. *Macromolecules* **1999**, *32*, 3136−3145.
(9) Doxastakis, M.; Kitsiou, M.; Fytas, G.; Theodorou, D. N.; Hadjichristidis, N.; Meier, G.; Frick, B. *J. Chem. Phys.* **2000**, *112*, 8687−8694.
(10) Min, B. C.; Qiu, X. H.; Ediger, M. D.; Pitsikalis, M.; Hadjichristidis, N. *Macromolecules* **2001**, *34*, 4466−4475.
(11) Haley, J. C.; Lodge, T. P.; He, Y. Y.; Ediger, M. D.; von Meerwall, E. D.; Mijovic, J. *Macromolecules* **2003**, *36*, 6142−6151.
(12) Zetsche, A.; Fischer, E. W. *Acta Polym.* **1994**, *45*, 168−175.
(13) Cendoya, I.; Alegria, A.; Alberdi, J. M.; Colmenero, J.; Grimm, H.; Richter, D.; Frick, B. *Macromolecules* **1999**, *32*, 4065−4078.
(14) Urakawa, O.; Sugihara, T.; Adachi, K. *Polym. Appl. (Jpn.)* **2002**, *51*, 10−17.
(15) Lartigue, C.; Guillermo, A.; CohenAddad, J. P. *J. Polym. Sci., Polym. Phys.* **1997**, *35*, 1095−1105.
(16) Lutz, T. R.; He, Y. Y.; Ediger, M. D.; Cao, H. H.; Lin, G. X.; Jones, A. A. *Macromolecules* **2003**, *36*, 1724−1730.
(17) Chin, Y. H.; Inglefield, P. T.; Jones, A. A. *Macromolecules* **1993**, *26*, 5372−5378.
(18) Composto, R. J.; Kramer, E. J.; White, D. M. *Macromolecules* **1988**, *21*, 2580−2588.
(19) Kim, E.; Kramer, E. J.; Osby, J. O. *Macromolecules* **1995**, *28*, 1979−1989.
(20) Urakawa, O.; Fuse, Y.; Hori, H.; Tran-Cong, Q.; Yano, O. *Polymer* **2001**, *42*, 765−773.
(21) Yang, X. P.; Halasa, A.; Hsu, W. L.; Wang, S. Q. *Macromolecules* **2001**, *34*, 8532−8540.
(22) Katana, G.; Fischer, E. W.; Hack, T.; Abetz, V.; Kremer, F. *Macromolecules* **1995**, *28*, 2714−2722.
(23) Haley, J. C.; Lodge, T. P. *J. Rheol.* **2004**, *48*, 463−486.
(24) Pathak, J. A.; Kumar, S. K.; Colby, R. H. *Macromolecules* **2004**, *37*, 6994−7000.
(25) Rizos, A. K.; Fytas, G.; Semenov, A. N. *J. Chem. Phys.* **1995**, *102*, 6931−6940.
(26) He, Y. Y.; Lutz, T. R.; Ediger, M. D. *Macromolecules* **2004**, *37*, 9889−9898.
(27) Leroy, E.; Alegria, A.; Colmenero, J. *Macromolecules* **2002**, *35*, 5587−5590.
(28) Ngai, K. L.; Roland, C. M. *Rubber Chem. Technol.* **2004**, *77*, 579−590.
(29) Roland, C. M. *Macromolecules* **1987**, *20*, 2557−2563.
(30) Lodge, T. P.; McLeish, T. C. B. *Macromolecules* **2000**, *33*, 5278−5284.
(31) He, Y. Y.; Lutz, T. R.; Ediger, M. D. *J. Chem. Phys.* **2003**, *119*, 9956−9965.
(32) He, Y. Y.; Lutz, T. R.; Ediger, M. D.; Lodge, T. P. *Macromolecules* **2003**, *36*, 9170−9175.
(33) Arendt, B. H.; Krishnamoorti, R.; Kornfield, J. A.; Smith, S. D. *Macromolecules* **1997**, *30*, 1127−1137.
(34) Zawada, J. A.; Ylitalo, C. M.; Fuller, G. G.; Colby, R. H.; Long, T. E. *Macromolecules* **1992**, *25*, 2896−2902.
(35) A recent model from Haley et al. based upon the Lodge/McLeish model is successful in anticipating the experimentally observed curvatures in plots of viscosity vs composition, and the predictions are in reasonable agreement with the data for several systems tested (ref 23).

(36) Chapman, B. R.; Hamersky, M. W.; Milhaupt, J. M.; Kostelecky, C.; Lodge, T. P.; von Meerwall, E. D.; Smith, S. D. *Macromolecules* **1998**, *31*, 4562−4573.
(37) Adachi, K.; Hirano, H. *Macromolecules* **1998**, *31*, 3958−3962.
(38) Roland, C. M.; Ngai, K. L.; Santangelo, P. G.; Qiu, X. H.; Ediger, M. D.; Plazek, D. J. *Macromolecules* **2001**, *34*, 6159−6160.
(39) He, Y. Y.; Lutz, T. R.; Ediger, M. D.; Ayyagari, C.; Bedrov, D.; Smith, G. D. *Macromolecules* **2004**, *37*, 5032−5039.
(40) Hadjichristidis, N.; Iatrou, H.; Pispas, S.; Pitsikalis, M. *J. Polym. Sci., Polym. Chem.* **2000**, *38*, 3211−3234.
(41) Kaplan, M. L.; Bovey, F. A.; Cheng, H. N. *Anal. Chem.* **1975**, *47*, 1703−1705.
(42) He, Y. Y.; Lutz, T. R.; Ediger, M. D. *Macromolecules* **2003**, *36*, 8040−8048.
(43) Lyerla, J. R.; Levy, G. C. *Top. Carbon-13 NMR Spectrosc.* **1974**, *1*, 79.
(44) Heatley, F. *Prog. Nucl. Magn. Reson. Spectrosc.* **1979**, *13*, 47−85.
(45) Heatley, F. *Annu. Rep. NMR Spectrosc.* **1986**, *17*, 179−230.
(46) Gisser, D. J.; Glowinkowski, S.; Ediger, M. D. *Macromolecules* **1991**, *24*, 4270−4277.
(47) Loewenstein, A. *Advances in Nuclear Quadrupole Resonance*; John Wiley & Sons: London, 1983; Vol. 5.
(48) Bandis, A.; Wen, W. Y.; Jones, E. B.; Kaskan, P.; Zhu, Y.; Jones, A. A.; Inglefield, P. T.; Bendler, J. T. *J. Polym. Sci., Polym. Phys.* **1994**, *32*, 1707−1717.
(49) Moe, N. E.; Qiu, X. H.; Ediger, M. D. *Macromolecules* **2000**, *33*, 2145−2152.
(50) Qiu, X. H.; Moe, N. E.; Ediger, M. D.; Fetters, L. J. *J. Chem. Phys.* **2000**, *113*, 2918−2926.
(51) Tammann, G.; Hesse, W. *Z. Anorg. Allg. Chem.* **1926**, *156*, 245.
(52) Williams, M. L.; Landel, R. F.; Ferry, J. D. *J. Am. Chem. Soc.* **1955**, *77*, 3701−3707.
(53) von Meerwall, E. D.; Ferguson, R. D. *Comput. Phys. Commun.* **1981**, *21*, 421−429.
(54) von Meerwall, E. D.; Kamat, M. *J. Magn. Reson.* **1989**, *83*, 309−323.
(55) von Meerwall, E. D.; Palunas, P. *J. Polym. Sci., Polym. Phys.* **1987**, *25*, 1439−1457.
(56) Shim, S. E.; Parr, J. C.; von Meerwall, E.; Isayev, A. I. *J. Phys. Chem. B* **2002**, *106*, 12072−12078.
(57) In the order of SISI23, SISI42, SISI60, SISI80, the input T_g for PI homopolymer in the Lodge/McLeish model is 210, 209, 205, 198 K; the input T_g for PS homopolymer is 317, 340, 345, 355 K. The values were calculated on the basis of the relationships between T_g and molecular weight cited in ref 36.
(58) For the PS component, no junction effect is included as we assume that there is no significant difference in the segmental dynamics between a free end group and an end group connected to a (much faster) PI chain. For the PI component, we assume that there are four repeat units near the junction point for which the segmental dynamics are significantly slowed by the connected PS chain. In the Lodge/McLeish model we replace eq 13 with eqs 7 and 8 in ref 32.
(59) Kant, R.; Kumar, S. K.; Colby, R. H. *Macromolecules* **2003**, *36*, 10087−10094.
(60) Lutz, T. R.; He, Y. Y.; Ediger, M. D.; Pitsikalis, M.; Hadjichristidis, N. *Macromolecules* **2004**, *37*, 6440−6448.
(61) Faller, R. *Macromolecules* **2004**, *37*, 1095−1101.
(62) For PB/PVE, an "object" solution of entangled PB in oligomeric PVE and a "mirror" solution of entangled PVE in oligomeric PB were studied (ref 21), and the friction coefficients of the entangled component in each type of blend were extracted. Thus, the terminal activation energies of PB and PVE in Figure 7 are not from the same blend.
(63) Tang, H.; Schweizer, K. S. *J. Chem. Phys.* **1996**, *105*, 779−791.
(64) Milhaupt, J. M.; Chapman, B. R.; Lodge, T. P.; Smith, S. D. *J. Polym. Sci., Polym. Phys.* **1998**, *36*, 3079−3086.
(65) Maconnachie, A.; Kambour, R. P.; White, D. M.; Rostami, S.; Walsh, D. J. *Macromolecules* **1984**, *17*, 2645−2651.
(66) In Figure 7 from left to right, the five systems have thermodynamic interaction parameters (χ) of −0.004, 0.002, −0.0002. 0.094, and −0.002 (refs 25 and 31).
(67) He, Y. Y. Dynamic Properties in Miscible Polymer Blends and Copolymers. Ph.D. Thesis, University of Wisconsin−Madison, 2005.
(68) Doxastakis, M.; Chrissopoulou, K.; Aouadi, A.; Frick, B.; Lodge, T. P.; Fytas, G. *J. Chem. Phys.* **2002**, *116*, 4707−4714.
(69) Friedman, E. M.; Porter, R. S. *Trans. Soc. Rheol.* **1975**, *19*, 493.
(70) Gordon, M.; Taylor, J. S. *J. Appl. Chem.* **1952**, *2*, 493.
(71) For the PI homopolymer, the line was obtained by fitting the combined diffusion results and normal mode relaxation data from dielectric relaxation measurements (not shown here) on the same sample. For the PS homopolymer, the line was extrapolated to high temperatures using the temperature dependence of the segmental dynamics (Figure 4). The uncertainty introduced by these two extrapolations is no more than 0.1 decade. The two thin solid lines are VTF fits to the homopolymer data and have the following VTF parameters: for PS, $\zeta_\infty = 5.4 \times 10^{-11}$ dyn s/cm, $T_0 = 280$ K, $B = 495$ K; for PI, $\zeta_\infty = 6.7 \times 10^{-11}$ dyn s/cm, $T_0 = 170$ K, $B = 393$ K.

MA0505225